

## Microstructure and Microhardness of an Al-Zr-Ti-Fe Alloy

Takashi Maeshima<sup>1</sup> and Hideaki Matsuoka<sup>1</sup>

<sup>1</sup>Toyota Central R&D Labs., Inc. 41-1 Yokomichi-St, Nagakute-cyo, AICHI 480-1192, JAPAN

The microstructure and microhardness of Al-0.3mol%Zr-0.5mol%Ti-2.0mol%Fe alloy were investigated. Fine-grained dual-phase microstructures were obtained, containing primary  $\alpha$ -Al and eutectic phase, by gravity casting using a Cu mold. The eutectic structures consisted of Al-Fe and  $\alpha$ -Al. Transmission electron microscopy (TEM) analysis revealed that the crystallization of rod shaped, meta-stable  $Al_6Fe$  phase still remained during aging at 723 K. Spherical and coherent  $Al_3(Zr, Ti)$  precipitates with the  $L1_2$  structure were observed in  $\alpha$ -Al using high-resolution electron transmission microscopic observations. A large increment in hardness was obtained by Fe-addition to the Al-Zr-Ti alloy. It is concluded that the addition of Fe to the Al-Zr-Ti alloy enhances its mechanical properties.

**Keywords:** *aluminum-zirconium-titanium-iron, precipitation strengthening,  $Al_3(Zr, Ti)$ ,  $L1_2$  type structure,  $Al_6Fe$  meta-stable phase.*

### 1. Introduction

Aluminum alloys are well known to have low density, high specific strength and corrosion resistance. They are therefore widely used for weight reduction in weight-sensitive structural components. The major strengthening method of most aluminum alloys is precipitation strengthening. However, the absence of thermal stability at high temperatures restricts their further applications. Thus, new aluminum alloys that possess high strength at room temperature along with good thermal stability are needed.

The binary Al-Zr alloy exhibits precipitation strengthening and thermal stability by aging. It is well known that the ordered structure,  $L1_2$  type  $Al_3Zr$  precipitates contribute to these properties. On prolonged aging at elevated temperatures, decomposition of supersaturated Al-Zr solid solutions occurs by the nucleation of  $Al_3Zr$  [1]. By substituting Ti for Zr,  $Al_3(Zr, Ti)$  precipitates exhibit a reduced coarsening rate compared to  $Al_3Zr$  precipitates. Similar phenomena have also been observed for other precipitates, such as  $Al_3(Sc, Zr)$  and  $Al_3(Zr, V)$  [2-6]. Recently, the particle morphologies and compositions of  $Al_3(Zr, Ti)$  precipitates in Al-0.3mol%Zr-0.5mol%Ti alloy were reported. The Al-Zr-Ti alloy exhibits nonuniform dendritic distribution of solute atoms in Zr and Ti solute-rich regions after casting. Spherical and coherent precipitates with diameters between 3 and 5nm were observed in aged Al-Zr-Ti alloy. The Zr:Ti ratio of the  $Al_3(Zr, Ti)$  precipitates decreased from the center to the interface in the radial direction [7].

However, further strengthening of the ternary Al-Zr-Ti alloy may be impossible because of the low solid solubility of the alloying elements Zr, Ti in Al. It is expected that the better strengthening will be obtained by Fe-addition for the Al-Zr-Ti alloy. Though Fe also has low solid solubility in Al, crystallization of meta-stable  $Al_6Fe$  may contribute to high strength of Fe-added Al-Zr-Ti alloy. The current study is distinguished from other studies devoted to solid solution strengthening by the supersaturated Al-Fe solid solution in the Al alloy [8]. This study focuses on the effective utilization of the meta-stable state of the Al-Fe phase.

In the present work, we investigated the microstructure and microhardness of Al-0.3mol%Zr-0.5mol%Ti-2.0mol%Fe alloy.

## 2. Experimental procedure

### 2.1 Materials preparation and aging conditions

Al-0.3mol%Zr-0.5mol%Ti and Al-0.3mol%-0.5mol%Ti-2.0mol%Fe alloys were investigated in this study. The alloys were employed by gravity casting with pure Al, Al-10mass%Zr, Al-10mass%Ti and Al-10mass%Fe master alloys. The Cu mold used in the present study and the specimen indicated by the shadow area are shown schematically in Fig. 1. The chemical compositions of Al-Zr-Ti and Al-Zr-Ti-Fe alloys are listed in Table 1. As-cast samples were aged directly, with no prior homogenization treatment. Aging was performed at temperatures between 573 and 773 K for 1 h in atmosphere.

### 2.2 Vickers hardness measurements and microstructural observations

The mechanical property of the as-cast and aged samples was evaluated by Vickers hardness tests. Vickers hardness was measured on polished samples and determined using the average value of 7 independent measurements.

The microstructure was investigated by scanning electron microscopy (SEM; Hitachi S-3600-N) and transmission electron microscopy (TEM; Hitachi HF-2200). TEM samples were prepared by mechanically thinning sections to a thickness of about 100  $\mu\text{m}$ . Discs of 3mm diameter were punched from these sections and thinned to perforation by twin-jet electro polishing using a solution of 70% methanol and 30% nitric acid. The thin foils were examined by TEM that was equipped with an energy dispersive X-ray spectroscopy (EDX; Thermo Scientific NORAN) detector.

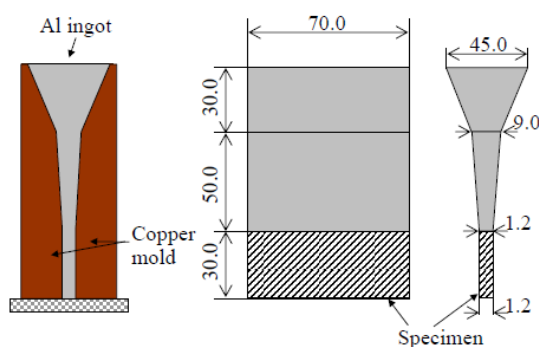


Fig. 1 Schematic diagram of the casting mold and an ingot specimen (mm).

Table 1 Chemical compositions of the specimens (mol%).

Specimen	Zr	Ti	Fe	Si	Mg	Al
Al-Zr-Ti	0.33	0.48	0.06	<0.05	<0.05	Balance
Al-Fe-Zr-Ti	0.31	0.50	2.12	<0.05	<0.05	Balance

## 3. Results and Discussion

Figure 2 displays Vickers hardness changes in the Al-Zr-Ti and Al-Zr-Ti-Fe alloys during the isochronal aging step (1h at each temperature). The hardness of the Al-Zr-Ti alloy exhibits three different regions: (a) incubation period; (b) a short transient period with rapid increase in hardness; and (c) a plateau period at high hardness. Compared to the Al-Zr-Ti alloy, the hardness of the Al-Zr-Ti-Fe alloy exhibits another region in addition to the above three regions, (d) a decrease of the hardness at high aging temperatures.

Figure 3 shows SEM backscattered electron images of the as-cast Al-Zr-Ti and Al-Zr-Ti-Fe alloys. The first solid to form during solidification is richer in Zr and Ti compared to the bulk alloy composition in the Al-Zr-Ti alloy. Therefore, the first solid regions exhibit lighter contrast depending on the Z-contrast from the backscattered electrons. The solute-poor interdendritic channels which exhibit darker contrast surround the solute-rich dendritic regions as shown in Fig. 3(a). In the Al-Zr-Ti-Fe alloy, the first solid to exhibit darker contrast is  $\alpha$ -Al, as shown in Fig. 3(b). The subsequently-crystallized eutectic structure which exhibits lighter contrast is comprised of Al-Fe

compounds and  $\alpha$ -Al. The eutectic structure is represented by the network-like microstructure surrounding primary  $\alpha$ -Al. The Al-Fe phase diagram shows quite narrow ranges of solubility in  $\alpha$ -Al (maximum 0.025mol%Fe) and is of the eutectic type with the eutectic point of Al-Al<sub>3</sub>Fe at 0.92mol%Fe in equilibrium. However, the  $\alpha$ -Al phase as a first solid followed by the eutectic structure was obtained in the crystallization of the 2.0mol%Fe added alloy in the present study. Rapid solidification using the Cu mold would yield the non-equilibrium microstructure of the Al-Zr-Ti-Fe alloy.

Figure 4 shows TEM bright field micrograph of Al-Zr-Ti-Fe alloy aged at 723 K. The aging condition of the TEM sample corresponds to the peak hardness shown in Fig. 2. The microstructure seems to remain unchanged from that of the as-cast alloy in this field of view. The eutectic structure has been observed in both (a) and (b) regions of Fig. 4. Therefore, the morphology of eutectic structure is not lamellar alignment but is rod-shaped Al-Fe phase surrounding the  $\alpha$ -Al phase. The morphology of eutectic structure was confirmed by tilting experiments in TEM. Rod-shaped Al-Fe phase with diameters between 100 and 300 nm and with lengths of several  $\mu$ m were observed. Figure 5 shows the eutectic structure obtained after the alloy aged at 723 K, along with the selected area diffraction pattern (SADP) and EDX analysis from the Al-Fe phase indicated by the arrow. The SADP in Fig. 5(b) is indexed as the meta-stable Al<sub>6</sub>Fe (orthorhombic,  $a_0 = 0.646$ ,  $b_0 = 0.744$ ,  $c_0 = 0.878$ ) [9]. The Al-Fe phase indicated by the arrow consisted of only Al and Fe as shown in Fig. 5(c). Figure 6 shows the primary  $\alpha$ -Al phase of the Al-Zr-Ti-Fe alloy aged at 723 K. Spherical precipitates with diameter of several nm were observed in the primary  $\alpha$ -Al phase as shown in Fig. 6(a). The SADP in Fig. 6(b) indicates a face-centered cubic  $\alpha$ -Al matrix and L1<sub>2</sub> ordered structure. It is clear that coherent precipitates form so that there is a definite relationship between the structures of matrix and the precipitate as indicated in Fig. 6(d). Al, Zr and Ti were detected in the precipitates, as shown in Fig. 6(e). Therefore, the precipitates are confirmed to be a composite L1<sub>2</sub>-type Al<sub>3</sub>(Zr, Ti). A small amount of Fe was also detected and the analysis was mainly attributed to solute Fe within the  $\alpha$ -Al matrix.

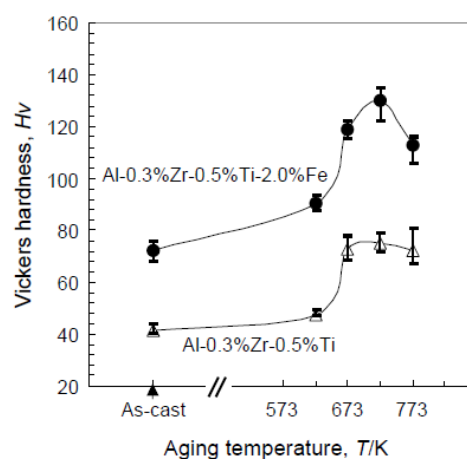


Fig. 2 Vickers hardness during isochronal aging (1h at each temperature) of Al-0.3%Zr-0.5%Ti and Al-0.3%Zr-0.5%Ti-2.0%Fe alloy.

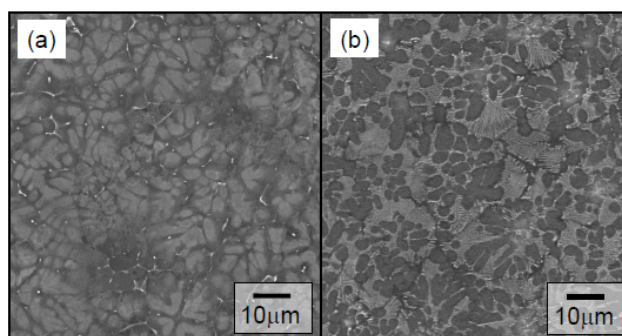


Fig. 3 Backscattered electron SEM images of as-cast (a) Al-0.3%Zr-0.5%Ti and (b) Al-0.3%Zr-0.5%Ti-2.0%Fe alloy.

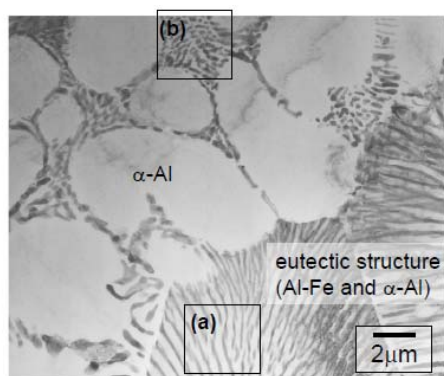


Fig. 4 Bright-field TEM micrograph of Al-0.3%Zr-0.5%Ti-2.0%Fe alloy aged at 723 K. The region marked (a) and (b) indicate the eutectic structure consisting of Al-Fe and  $\alpha$ -Al.

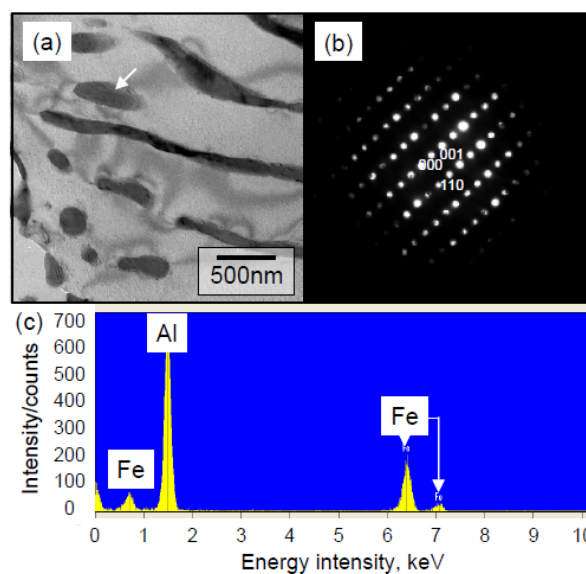


Fig. 5 TEM micrograph of Al-0.3%Zr-0.5%Ti-2.0%Fe alloy aged at 723 K. (a) Bright-field TEM image; (b) micro-beam diffraction pattern obtained from the Al-Fe phase indicated by the arrow, and (c) EDX analysis of Al-Fe phase indicated by the arrow.

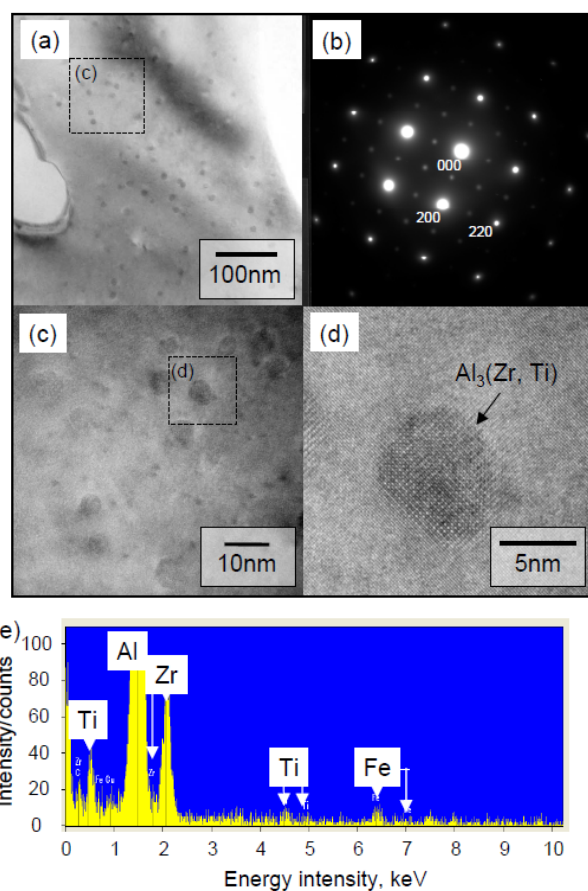


Fig. 6 TEM micrograph of Al-0.3%Zr-0.5%Ti-2.0%Fe alloy aged at 723 K. (a) Bright-field TEM image; (b) SADP of (a); (c, d) HREM micrographs and (e) EDX analysis of  $\text{Al}_3(\text{Zr, Ti})$  precipitates indicated by the arrow.

The increase in the hardness with aging of both the Al-Zr-Ti and Al-Zr-Ti-Fe alloy in Fig. 2 is attributed to the precipitation strengthening by  $\text{Al}_3(\text{Zr}, \text{Ti})$ . However, the hardness change behavior of both alloys differed slightly, even though both alloys contained almost the same amount of Zr and Ti as shown in Table 1. The difference in hardness between Al-Zr-Ti and Al-Zr-Ti-Fe as-cast alloys was as a result of the network-like eutectic structure which consisted of  $\alpha$ -Al and  $\text{Al}_6\text{Fe}$ . The increment in hardness of the Al-Zr-Ti-Fe alloy was larger than that of the Al-Zr-Ti alloy at the peak hardness which corresponds to the hardness of both alloys aged at 723 K. The increment in hardness of the 723 K aging point of the Al-Zr-Ti-Fe alloy could not be explained from the microstructural analysis in the current study. The hardness of the Al-Zr-Ti alloy exhibits a plateau region between 673 K and 773 K aging, while the hardness of the Al-Zr-Ti-Fe alloy exhibits a rapid decrease in the 773 K-aged alloy from the peak for 723 K-aged alloy. This decrease was probably caused by phase transformation in the Al-Fe phase. The meta-stable  $\text{Al}_6\text{Fe}$  in the Al alloy transforms to the stable  $\text{Al}_3\text{Fe}$  by holding at 623 K or above for a certain periods of time [10, 11]. It is expected that the  $\text{Al}_6\text{Fe}$  will transform to  $\text{Al}_3\text{Fe}$  during aging at 773 K, yet the meta-stable  $\text{Al}_6\text{Fe}$  was observed in the Al-Zr-Ti-Fe as-cast alloy and the aging alloy at 723 K in this study.

#### 4. Summary

The microstructure and microhardness of Al-0.3mol%Zr-0.5mol%Ti-2.0mol%Fe alloy were investigated. The following results were obtained and discussed:

- The primary  $\alpha$ -Al and eutectic structure were observed in the crystallization of the as-cast Al-Zr-Ti-Fe alloy. The eutectic structure which consists of rod-shaped meta-stable  $\text{Al}_6\text{Fe}$  and  $\alpha$ -Al is represented by a network-like microstructure surrounding the primary  $\alpha$ -Al.
- Spherical and coherent  $\text{Al}_3(\text{Zr}, \text{Ti})$  precipitates with the  $\text{L}1_2$  structure were formed in  $\alpha$ -Al upon aging at 723 K for 1 h leading to peak hardness. The  $\text{Al}_6\text{Fe}$  phase within the eutectic structure remains in meta-stable phase instead of transforming to  $\text{Al}_3\text{Fe}$  during aging at 723 K.
- A large increment in hardness obtained by Fe-addition to the Al-Zr-Ti alloy.

#### References

- [1] M. Furukawa, H. B. Wang and M. Nemoto: JILM. Vol. 40 (1990) pp. 20-26.
- [2] T. Sato, A. Kamio and G. W. Lorimer: Materials Science Forum Vol. 217-222 (1996), pp. 895-900.
- [3] S. C. Chung, S. Z. Han, H. M. Lee and H. S. Kwon: Scripta Metall. et Mater. Vol. 33 (1995) pp. 687-693.
- [4] S. Iwamura and Y. Miura: JILM. Vol. 56 (2006), pp. 100-104.
- [5] M. S. Zedalis and M. E. Fine: Metall. Trans. A Vol. 17 (1986), pp. 2187-2198.
- [6] K. E. Knippling, D. C. Dunand and D. N. Seidman: Microscopy and Microanalysis Vol.13 (2007), pp. 503-516.
- [7] T. Maeshima and H. Masuoka: Materials Science Forum Vols. 638-642 (2010), pp.279-284.
- [8] H. Sasaki, K. Kita, J. Nagahora and A. Inoue: Mater. Trans. Vol. 42 (2001), pp. 1561-1565.
- [9] L. K. Walford: Acta Crystallogr. 18 (1965) pp. 287-291.
- [10] H. Kosuge and H. Takada: JILM. Vol. 19 (1979) pp. 64-69.
- [11] H. Suzuki, M. Kannno, H. Tanabe and K. Itoi: JILM. Vol. 28 (1978) pp. 284-291.